Analytic calculation of linear susceptibility in velocity-dependent pump-probe spectroscopy

Geol Moon and Heung-Ryoul Noh*
Department of Physics and Institute of Opto-Electronic Science and Technology, Chonnam National University, Gwangju 500-757, Korea
(Received 12 May 2008; published 4 September 2008)

We present an analytic calculation for linear susceptibility in pump-probe spectroscopy for a Doppler broadened atomic vapor. The analytic form of the population of each magnetic sublevel of a ^{87}Rb atom, illuminated by a weak circularly polarized pump beam, was calculated for the lowest order of laser intensity and used in the calculation for the susceptibility of a counterpropagating (copropagating) probe beam. The obtained analytic results for the susceptibility can be used for calculating the absorption or the refractive index of the probe beam as functions of pump beam diameter and intensity.

DOI: 10.1103/PhysRevA.78.032506 PACS number(s): 32.30.−r, 42.62.Fi, 32.70.Jz

I. INTRODUCTION

In high resolution laser spectroscopy for a Doppler broadened atomic vapor, such as saturated absorption spectroscopy (SAS) [1–3] or polarization spectroscopy (PS) [1,4,5], sub-Doppler resolution originated from the fact that atoms belonging to a specific velocity group could interact with counterpropagating pump and probe beams simultaneously. Since these spectroscopic techniques are very simple and efficient, although sub-Doppler resolution can be obtained from laser cooled atoms [6], these are still widely used in many laboratories for locking of laser frequency [7]. In the case of elements possessing complicated level structures such as alkali-metal atoms, SAS or PS spectra are significantly influenced by velocity selective optical pumping (VSOP) [3,8,9]. When two different laser fields are employed unlike SAS or PS where the pump and probe lasers are derived from a laser, as well as VSOP, new interesting phenomena such as electromagnetically induced transparency (EIT) [10,11] or coherent population trapping (CPT) [12] are observed. There are excellent studies on these subjects for developing applications such as lasing without inversion [13], enhancement of the refractive index [14], light storage [15], and quantum-information processing [16].

Besides the phenomena which necessitate atomic coherence such as EIT or CPT, the use of two independent lasers enables us to observe interesting spectra such as elimination of crossover resonances by using two copropagating pump and probe beams [17]. Recently, there have been many reports on VSOP spectra observed in dilute atomic vapor [18–27]. Ghosh *et al.* reported experimental observation of velocity-selective resonance dips for the ^{85}Rb D_2 transition line [21] and explained VSOP spectra by simulation for a five-level system [25–27]. They also reported observation of EIT signal superposed on VSOP spectra of the ^{85}Rb D_2 line [22]. In addition, the coherence effects observed in VSOP spectra were reported for Na [20], Li [23], and ^{85}Rb [24] atoms. Although the measured spectra were well understood by simple calculation, to our knowledge, there have been no reports on studies of nonstationary phenomena, systematic study on the dependence of polarization of the used laser beams, or accurate analytic solutions for the spectra.

Recently, we reported on analytic calculations of the spectra of SAS [28] and PS [29]. Extending the previous reports further, in this paper, we present a theoretical study on analytic calculations for the susceptibility (χ) in pump-probe spectroscopy for a Doppler broadened vapor cell. Once χ is known, the birefringence (refractive index, n) and dichroism (absorption coefficient, α) can be obtained by the following equations [30]:

$$n \simeq 1 + \tfrac{1}{2}\,\mathrm{Re}\,\chi, \quad \alpha \simeq k\,\mathrm{Im}\,\chi,$$

where k is the wave vector. Using the methods developed in our study described in this paper, as far as weak pump beam intensity is concerned, the analytic VSOP spectra depending on various polarization configurations ($\sigma^{\pm}$ or π polarization for the pump and arbitrary polarization for the probe beam), pump beam intensity, and the diameter of the pump beam, i.e., a nonstationary effect can be obtained. Since we are interested in the situation of weak pump beam intensity, nonlinear phenomena such as EIT or four-wave mixing are not shown [18,20].

This paper is organized as follows. In Sec. II, we present a method for calculation of the susceptibility for ^{87}Rb atoms. In Sec. III, we present the results of the calculation and the explicit form of the analytic results for a specific experimental scheme. In the final section, we summarize the results.

II. THEORY

We consider the D_2 transition of ^{87}Rb atoms. As shown in Fig. 1, the pump (σ^+ polarized) and probe beams overlap in a vapor cell in counterpropagating or copropagating schemes. Because the pump and probe beams are tuned at the transition line from the lower or upper ground states, we consider four schemes as depicted in Fig. 1. We define the angular momentum quantum number of the ground state where the pump (probe) beam is tuned as F_p (F). As discussed in previous reports, we assume that the energy spacings of the excited state are much larger than the natural linewidth so that the off-resonant transition might be neglected [28,29].

*hrnoh@chonnam.ac.kr

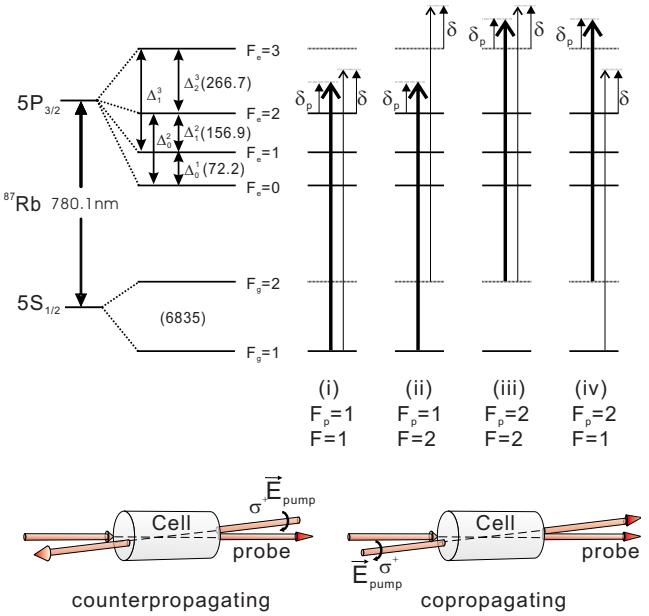

FIG. 1. (Color online) The energy level diagram of the ^{87}Rb atom (top). The thick (thin) lines denote the pump (probe) laser beam. The frequencies are shown in units of MHz. A schematic for velocity-selective optical pumping spectroscopy (bottom). The pump beam is σ^+ polarized and propagates along or opposite to the probe beam's propagation direction.

When an atom interacts with pump and probe beams, the internal dynamics of the atom is described by the following density matrix equation:

$$\dot{\rho} = -\frac{i}{\hbar}[H_0 + V_{\mathrm{pu}} + V_{\mathrm{pr}}, \rho] + (\dot{\rho})_{\mathrm{sp}}, \tag{1}$$

where ρ is the density operator, H_0 and V_{pu} (V_{pr}) are the bare atomic and interaction Hamiltonians with the pump (probe) beam, respectively. $(\dot{\rho})_{\mathrm{sp}}$ represents the spontaneous decay terms. To obtain the induced polarizability, we decompose a density matrix element ρ_{eg} between the magnetic sublevels $|e\rangle$ and $|g\rangle$ belonging to the excited and ground states, respectively, as follows:

$$\rho_{eg} = \rho_{eg}^{(\mathrm{pu})} e^{-i\omega_{\mathrm{pu}}t} + \rho_{eg}^{(\mathrm{pr})} e^{-i\omega_{\mathrm{pr}}t}. \tag{2}$$

In Eq. (2), $\omega_{\mathrm{pu}} = \omega_p \pm k_p v$ and $\omega_{\mathrm{pr}} = \omega - kv$ are the frequencies of the pump and probe beams experienced by an atom moving with a velocity v where the sign + (−) implies the counterpropagating (copropagating) scheme, and k_p and ω_p (k and ω) are the wave vector and the angular frequency of the pump (probe) beam, respectively. Then, we have the following results:

$$\rho_{eg}^{(\mathrm{pr})} = -\frac{\langle e|D|g\rangle E_{\mathrm{pr}}}{i\hbar\Gamma + 2[\hbar\omega_{\mathrm{pr}} - (E_e - E_g)]}(\rho_{gg} - \rho_{ee}), \tag{3}$$

where D is the dipole operator and E_{pr} is the amplitude of the electric field of the probe beam, Γ is the decay rate of the excited state, and $E_g(E_e)$ is the energy of the ground (excited) state. Since the intensity of the probe beam is much weaker than that of the pump beam, the probe beam is neglected in the calculation of ρ_{ee} or ρ_{gg} in Eq. (3). The susceptibility is calculated from the polarizability $P^{(\mathrm{pr})} = N\,\mathrm{Tr}(\rho D)$ averaged over the Maxwell-Boltzmann velocity distribution, and is given by

$$\chi = -\int_{-\infty}^{\infty} dv \frac{3\lambda^3}{4\pi^2}\frac{N}{\sqrt{\pi}u} e^{-(v/u)^2} \times \sum_{F_e=F-1}^{F+1}\sum_{m=-F}^{F} \frac{R_{F,m}^{F_e,m+1}(P_F^m - Q_{F_e}^{m+q})}{i + 2(\delta - kv + \Delta_{F_e}^{F+1})/\Gamma}, \tag{4}$$

where N is the atomic density, $u = (2k_BT/M)^{1/2}$ is the most probable velocity with M the mass of a ^{87}Rb atom, λ is the resonance wavelength, δ is the detuning of the probe beam with respect to the transition $F_g = F \rightarrow F_e = F+1$, q represents the polarization of the probe beam, $\hbar\Delta_{F_{e_1}}^{F_{e_2}} = E_{F_{e_2}} - E_{F_{e_1}}$ is the hyperfine energy spacing of the excited states, and $P_{F_g}^{m_g}(Q_{F_e}^{m_e})$ is the population of the ground (excited) state $|F_g, m_g\rangle(|F_e, m_e\rangle)$. In Eq. (4), the normalized transition strength is given by [31]

$$R_{F_g,m_g}^{F_e,m_e} = (2L_e+1)(2J_e+1)(2J_g+1)(2F_e+1)(2F_g+1) \times \left[\begin{Bmatrix} L_e & J_e & S \\ J_g & L_g & 1 \end{Bmatrix}\begin{Bmatrix} J_e & F_e & I \\ F_g & J_g & 1 \end{Bmatrix} \times \begin{pmatrix} F_g & 1 & F_e \\ m_g & m_e - m_g & -m_e \end{pmatrix}\right]^2,$$

where L, S, and I denote the orbital, electron spin, and nuclear spin angular momenta, respectively. $\{\cdots\}$ and $(\cdots)$ represent the $6J$ and $3J$ symbols, respectively.

To calculate the susceptibility in Eq. (4), we must know the analytic forms of the populations. We refer to Refs. [28,29] for the detailed calculation of the populations. The population of the ground state is decomposed as

$$P_F^m = P_{F_p\rightarrow F_p+1}^{(F,m)}(\delta_p \pm k_p v) + P_{F_p\rightarrow F_p}^{(F,m)}(\delta_p + \Delta_{F_p}^{F_p+1} \pm k_p v) + P_{F_p\rightarrow F_p-1}^{(F,m)}(\delta_p + \Delta_{F_p-1}^{F_p+1} \pm k_p v) - \frac{2}{2(2I+1)}, \tag{5}$$

where $P_{F_p\rightarrow\mu}^{(F,m)}(\Delta)$ is the population of the ground state $|F,m\rangle$ when the frequency of the pump beam is tuned near the transition $F_p \rightarrow \mu$, and δ_p is the detuning of the pump beam relative to the transition $F_g = F_p \rightarrow F_e = F_p + 1$. In the calculation of Eq. (4), all of the excited-state populations are neglected except for Q_3^3 of the ^{87}Rb atoms [28,29]. Then, Eq. (4) becomes the following equation:

$$\chi = -\sum_{m=-F}^{F}\int_{-\infty}^{\infty} dv \frac{3\lambda^3}{4\pi^2}\frac{N}{\sqrt{\pi}u}e^{-(v/u)^2}\left(\frac{R_{F,m}^{F+1,m+q}}{i+2(\delta-kv)/\Gamma}\right.$$
$$+\frac{R_{F,m}^{F,m+q}}{i+2(\delta+\Delta_F^{F+1}-kv)/\Gamma}+\frac{R_{F,m}^{F-1,m+q}}{i+2(\delta+\Delta_{F-1}^{F+1}-kv)/\Gamma}\Big)$$
$$\times\left(P_{F_p\to F_p+1}^{(F,m)}(\delta_p\pm k_pv)+P_{F_p\to F_p}^{(F,m)}(\delta_p+\Delta_{F_p}^{F_p+1}\pm k_pv)\right.$$
$$\left.+P_{F_p\to F_p-1}^{(F,m)}(\delta_p+\Delta_{F_p-1}^{F_p+1}\pm k_pv)-\frac{2}{2(2I+1)}\right). \quad (6)$$

In calculating Eq. (6), we must calculate the integration as given by

$$I_0 = -\int_{-\infty}^{\infty} dv \frac{3\lambda^3}{4\pi^2}\frac{N}{\sqrt{\pi}u}e^{-(v/u)^2}\frac{P_{F\to\mu}^m(C_2\pm k_pv)}{i+2(C_1-kv)/\Gamma}, \quad (7)$$

where C_1 and C_2 are constants composed of various detunings. As presented in Refs. [28,29], $P_{F_p\to\mu}^{(F,m)}(\Delta)$ is composed of four types of elements such as (i) k_1, (ii) $k_1\exp[-k_2s(\Delta)\Gamma t]$, (iii) $k_1s(\Delta)\Gamma t\exp[-k_2s(\Delta)\Gamma t]$, and (iv) $[p_3+p_4s(\Delta)]/[p_1+p_2s(\Delta)]$, where $s(\Delta)=s_0/(1+4\Delta^2/\Gamma^2)$ with $s_0=2(\Omega/\Gamma)^2$ and Ω is the Rabi frequency of the pump beam. The terms k_1, k_2, p_1, p_2, p_3, and p_4 are constants.

(i) When $P_{F\to\mu}^m(\Delta)=k_1$, Eq. (7) is given by

$$I_0 = ik_1C_0\exp[-(C_1/ku)^2],$$
$$C_0 = \frac{3\lambda^3}{4\pi^2}\frac{N}{\sqrt{\pi}u}\frac{\pi\Gamma}{2k}. \quad (8)$$

(ii) When $P_{F\to\mu}^m(\Delta)=k_1\exp[-k_2s(\Delta)\Gamma t]$, Eq. (7) becomes

$$I_0 = -\frac{3\lambda^3}{4\pi^2}\frac{N}{\sqrt{\pi}u}\exp[-(C_1/ku)^2]$$
$$\times\int_{-\infty}^{\infty} dv\frac{k_1}{i+2(C_1-kv)/\Gamma}\exp\left(-\frac{k_2s_0\Gamma t}{1+\frac{4}{\Gamma^2}(C_2\pm k_pv)^2}\right)$$
$$= C_0\exp\left[-\left(\frac{C_1}{ku}\right)^2\right]k_1\left[i+L\left(\frac{(k_p/k)C_1\pm C_2}{\Gamma},k_2s_0\Gamma t\right)\right], \quad (9)$$

where

$$L(a,b) = -i-\frac{2}{\pi}\int_{-\infty}^{\infty}\frac{1}{i+2y}\exp\left(-\frac{b}{1+4\left(a-\frac{k_p}{k}y\right)^2}\right)dy. \quad (10)$$

In Eq. (9), we have used the fact that $ku\gg\Gamma$. As was validated in Refs. [28,29], using an approximation given by

$$\exp\left(-\frac{b}{1+4\left(a-\frac{k_p}{k}y\right)^2}\right)\cong 1-\frac{b}{1+b+4\left(a-\frac{k_p}{k}y\right)^2},$$

we have

$$L(a,b)\simeq\frac{b}{\sqrt{b+1}}\frac{1}{2a+i\left(\frac{k_p}{k}+\sqrt{b+1}\right)}. \quad (11)$$

Since $k\simeq k_p$, we set $k_p/k\simeq 1$ in Eqs. (9) and (11), and in what follows.

(iii) When $P_{F\to\mu}^m(\Delta)=k_1s(\Delta)\Gamma t\exp[-k_2s(\Delta)\Gamma t]$, we have

$$I_0 = -C_0\exp[-(C_1/ku)^2]\frac{k_1}{k_2}L\left(\frac{C_1\pm C_2}{\Gamma},k_2s_0\Gamma t\right). \quad (12)$$

(iv) Finally, when $P_{F\to\mu}^m(\Delta)=[p_3+p_4s(\Delta)]/[p_1+p_2s(\Delta)]$,

$$I_0 = -\frac{3\lambda^3}{4\pi^2}\frac{N}{\sqrt{\pi}u}\exp[-(C_1/ku)^2]\int_{-\infty}^{\infty}dv\left(\frac{k_1}{i+2(C_1-kv)/\Gamma}\right.$$
$$\left.\times\frac{p_3+p_4s_0[1+4(C_2\pm kv)^2/\Gamma^2]^{-1}}{p_1+p_2s_0[1+4(C_2\pm kv)^2/\Gamma^2]^{-1}}\right)$$
$$= C_0\exp\left[-\left(\frac{C_1}{ku}\right)^2\right]$$
$$\times\left[i\frac{p_3}{p_1}-\left(\frac{p_4}{p_2}-\frac{p_3}{p_1}\right)L\left(\frac{C_1\pm C_2}{\Gamma},\frac{p_2}{p_1}s_0\right)\right]. \quad (13)$$

Using the results of Eqs. (8), (9), (12), and (13), Eq. (6) becomes the following equation:

$$\chi = \chi_{\mathrm{BG}}+C_0\sum_{\nu=F-1}^{F+1}D_\nu^{F+1}\sum_{\mu=F_p-1}^{F_p+1}\sum_{m=-F}^{F}R_{F,m}^{\nu,m+q}$$
$$\times M_{F_p\to\mu}^{(F,m)}[\delta+\Delta_\nu^{F+1}\pm(\delta_p+\Delta_\mu^{F_p+1})], \quad (14)$$

where the values $M_{F_p\to\mu}^{(F,m)}(\Delta)$ for all possible transitions are presented in the Appendix, and the Doppler factor is given by

$$D_n^m = \exp\left[-\left(\frac{\delta+\Delta_n^m}{ku}\right)^2\right]. \quad (15)$$

In Eq. (14), χ_{BG} represents the background susceptibility explicitly given by

$$\chi_{\mathrm{BG}} = \frac{i}{8}C_0(k_1D_{F+1}^{F+1}+k_2D_F^{F+1}+k_3D_{F-1}^{F+1}), \quad (16)$$

where $k_1=\frac{5}{6}(\frac{7}{3})$, $k_2=\frac{5}{6}(\frac{5}{6})$, $k_3=\frac{1}{3}(\frac{1}{6})$ for $F=1(2)$ for the ^{87}Rb atoms. In Eq. (16), the effect of the probe beam intensity was neglected.

III. RESULTS

The locations of the resonance signals in the spectra are determined by the following equation as can be known from Eq. (14),

$$\delta = \mp\delta_p\mp\Delta_\mu^{F_p+1}-\Delta_\nu^{F+1}, \quad (17)$$

where the upper (lower) sign denotes the counterpropagating (copropagating) scheme, $\mu=F_p+1,F_p,F_p-1$, and $\nu=F+1,F,F-1$. Easy identification can be made graphically as depicted in Fig. 2. Figures 2(a) and 2(b) show the results for

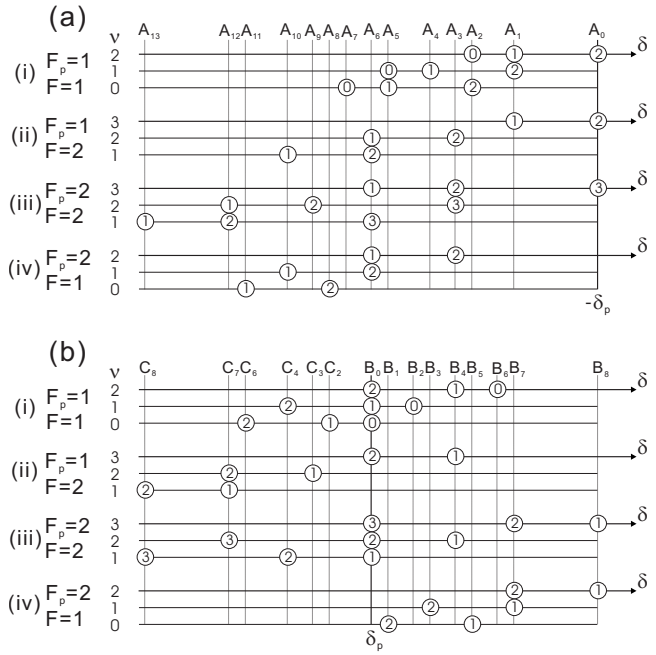

FIG. 2. The location of the resonance signals in (a) counterpropagating and (b) copropagating schemes. The circles lying in a specific vertical line represent the velocity groups contributing to the equal signal.

the counterpropagating and copropagating schemes, respectively, where the integers in circles denote μ. In Fig. 2, the circles lying in a specific vertical line contribute to the signal with the same detuning of the probe beam.

In Fig. 2(a), the displacements of the frequencies relative to $\delta=-\delta_p$ are given by the following:

$$A_0=0,\quad A_1=-\Delta_1^2,\quad A_2=-\Delta_0^2,\quad A_3=-\Delta_2^3,$$

$$A_4=-2\Delta_1^2,\quad A_5=-(2\Delta_1^2+\Delta_0^1),\quad A_6=-\Delta_1^3,$$

$$A_7=-2\Delta_0^2,\quad A_8=-\Delta_0^3,\quad A_9=-2\Delta_2^3,$$

$$A_{10}=-(\Delta_1^3+\Delta_1^2),\quad A_{11}=-(\Delta_1^3+\Delta_0^2),$$

$$A_{12}=-(2\Delta_2^3+\Delta_1^2),\quad A_{13}=-2\Delta_1^3.$$

The positions of the frequencies with respect to $\delta=\delta_p$ for the copropagating scheme in Fig. 2(b) are given as

$$B_0=0,\quad B_1=\Delta_2^3-\Delta_0^2,\quad B_2=\Delta_0^1,$$

$$B_3=\Delta_2^3-\Delta_1^2,\quad B_4=\Delta_1^2,\quad B_5=\Delta_2^3-\Delta_0^1,$$

$$B_6=\Delta_0^2,\quad B_7=\Delta_2^3,\quad B_8=\Delta_1^3,$$

and $C_n=-B_n$ for $n=2,\ldots,8$ with C_5 missing.

We can obtain the susceptibility spectra for all possible transition schemes using Eq. (14). For instance, we present the explicit analytic form of the calculated susceptibility for $F_p=2$ and $F=1$ in a copropagating scheme where both the pump and probe beams are σ^+ polarized as follows:

$$\chi(\delta)=\chi_{\mathrm{BG}}+C_0[D_2^2S_1(\delta-\delta_p-\Delta_1^3)+D_2^2S_{2a}(\delta-\delta_p-\Delta_2^3)+D_1^2S_{2b}(\delta-\delta_p-\Delta_2^3)+D_0^2S_3(\delta-\delta_p-\Delta_2^3+\Delta_0^1)+D_1^2S_4(\delta-\delta_p-\Delta_2^3+\Delta_1^2)+D_0^2S_5(\delta-\delta_p-\Delta_2^3+\Delta_0^2)], \tag{18}$$

where

$$S_1(\Delta)=-\frac{2145}{47\,488}L\left(\frac{\Delta}{\Gamma},\frac{59}{7200}\tau\right)-\frac{275}{8064}L\left(\frac{\Delta}{\Gamma},\frac{19}{800}\tau\right)-\frac{295}{17\,172}L\left(\frac{\Delta}{\Gamma},\frac{9}{200}\tau\right),$$

$$S_{2a}(\Delta)=-\frac{103}{784}L\left(\frac{\Delta}{\Gamma},\frac{5}{72}\tau\right)+\frac{149}{21\,168}L\left(\frac{\Delta}{\Gamma},\frac{3}{32}\tau\right),$$

$$S_{2b}(\Delta)=-\frac{3575}{142\,464}L\left(\frac{\Delta}{\Gamma},\frac{59}{7200}\tau\right)-\frac{375}{15\,232}L\left(\frac{\Delta}{\Gamma},\frac{19}{800}\tau\right)-\frac{54\,575}{1\,167\,696}L\left(\frac{\Delta}{\Gamma},\frac{9}{200}\tau\right),$$

$$S_3(\Delta)=-\frac{25}{1224}L\left(\frac{\Delta}{\Gamma},\frac{19}{800}\tau\right)-\frac{25}{1377}L\left(\frac{\Delta}{\Gamma},\frac{9}{200}\tau\right),$$

$$S_4(\Delta)=-\frac{1}{16}L\left(\frac{\Delta}{\Gamma},\frac{5}{72}\tau\right)-\frac{5}{216}L\left(\frac{\Delta}{\Gamma},\frac{3}{32}\tau\right),$$

$$S_5(\Delta)=-\frac{1}{70}L\left(\frac{\Delta}{\Gamma},\frac{5}{72}\tau\right)-\frac{5}{1512}L\left(\frac{\Delta}{\Gamma},\frac{3}{32}\tau\right), \tag{19}$$

where $\tau=s_0\Gamma t$.

The result of Eq. (18) is shown in Fig. 3, where $\delta_p=-\Delta_2^3-\frac{1}{2}\Delta_1^2$ and $\Omega=0.3\Gamma$. The average time $t=(\sqrt{\pi}/2)d/u$ was used, where $d(=3$ mm) is the pump beam diameter and u is the most probable velocity [32]. In Fig. 3(a), the black (A), red (B), and green (C) curves denote the real, imaginary, and background-subtracted imaginary part of the susceptibility, respectively. In Fig. 3, we can see that the signals are located at the position expected from the calculation. The positions of the five signals are $\delta=\Delta_1^2/2$, $-\Delta_1^2/2$, $-\Delta_1^2/2-\Delta_0^1$, $-\Delta_1^2/2-\Delta_1^2$, and $-\Delta_1^2/2-\Delta_0^2$ corresponding to S_1, $S_{2a}(S_{2b})$, S_3, S_4, and S_5, respectively. Figure 3(b) shows the transition scheme for each resonance signal. In Fig. 3(b), the thick (thin) arrows denote the pump (probe) beam. The small red arrows represent the frequency shift due to the Doppler effect, $kv=\pm\Delta_1^2/2$. We can see that the velocity group of $v=+[-]\Delta_1^2/(2k)$ contributes to the signals S_{2a}, S_4, and S_5 [S_1, S_{2b}, and S_3]. At the condition for S_{2a} and S_{2b}, the pump and probe beams constitute a Λ-type EIT configuration. However, the intensity of the pump and probe beams in our system are too weak to exhibit an EIT signal. If the intensity of both beams increases, a sharp dip occurs at S_{2a} and S_{2b} [22].

Figure 4 shows spectra of the imaginary part of the susceptibility for some typical experimental schemes. Panels

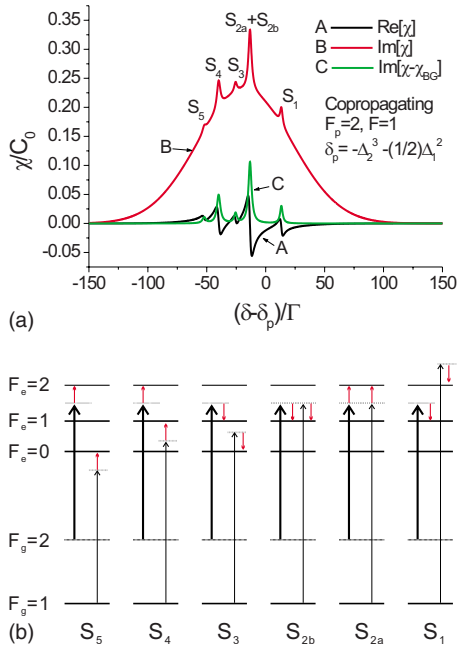

FIG. 3. (Color online) (a) The calculated susceptibility for $F_p=2$ and $F=1$ in a copropagating scheme where both the pump and probe beams are σ^+ polarized. (b) The transition scheme responsible for each resonance signal.

(a1), (a2), (a3), and (a4) [(b1), (b2), (b3), and (b4)] in Fig. 4 show the results for the scheme (i), (ii), (iii), and (iv), respectively, in the counterpropagating (copropagating) scheme. The frequency of the pump beam was tuned resonantly at $F_g=1 \rightarrow F_e=2$ [$F_g=2 \rightarrow F_e=3$] for the schemes (i) and (ii) [(iii) and (iv)], i.e., $\delta_p=0$, and that of the probe beam was scanned. The Rabi frequency of the pump beam was $\Omega=0.3\Gamma$. We can see that the signals are located at the detunings expected from Eq. (14). If δ_p varies, the resonance signals shift in accordance with Eq. (17).

IV. SUMMARY AND CONCLUSIONS

The spectra of the susceptibility for velocity-selective optical pumping in a counterpropagating (copropagating) scheme was analytically calculated [Eq. (14)]. We assumed that the intensity of the pump beam was much smaller than the saturation intensity, the pump beam was σ^+ polarized, and the polarization of the probe beam was arbitrary. It is also possible to obtain the results for other polarizations of the pump beam such as σ^- or π. Since the susceptibility was obtained as a function of time, which is equivalent to the beam size, we can obtain the spectra depending on the pump beam size. The signals for the real (imaginary) part consist of a finite number of dispersive (Lorentzian) functions with different amplitudes and widths. Each resonance signal results from specific velocity groups. To the best of our knowledge, accurate analytic results for the susceptibility of VSOP spectra have not been reported previously. In the calculation of the spectra, the effect of light pressure from a pump laser beam was not taken into account, resulting in a slight modification of the signals [33,34]. The obtained analytic results of the susceptibility can be used for easy prediction of the spectra in many experimental situations.

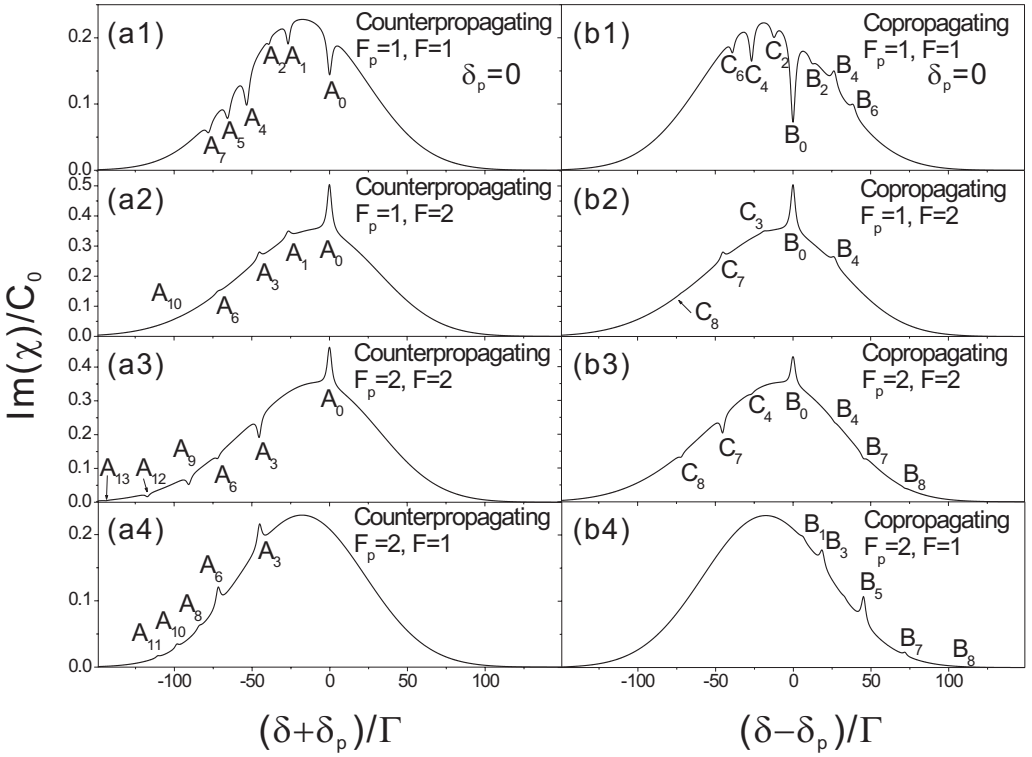

FIG. 4. The imaginary part of the susceptibility where $\delta_p=0$. Panels (a1), (a2), (a3), and (a4) [(b1), (b2), (b3), and (b4)] represent the results for the schemes (i), (ii), (iii), and (iv), respectively, in the counterpropagating (copropagating) scheme.

ACKNOWLEDGMENT

This work was supported by the Ministry of Commerce, Industry and Energy of Korea through the Industrial Technology Infrastructure Building Program.

APPENDIX

$M_{F_p\to\mu}^{(F,m)}(\Delta)$ are presented as follows. $M_{F_p\to\mu}^{(F,m)}$ and $L(b)$ are the simple notations for $M_{F_p\to\mu}^{(F,m)}(\Delta)$ and $L(\frac{\Delta}{\Gamma},b)$ with $\tau=s_0\Gamma t$, respectively. In Eq. (A3), $K\delta_{1,q}$ denotes the Kronecker δ symbol with q representing the polarization of the probe beam.

(i) When $F_p=1$ and $F=1$,

$$M_{1\to2}^{(1,-1)}=\frac{1}{8}L\left(\frac{11}{288}\tau\right),$$

$$M_{1\to2}^{(1,0)}=\frac{1}{32}L\left(\frac{11}{288}\tau\right)+\frac{3}{32}L\left(\frac{3}{32}\tau\right),$$

$$M_{1\to2}^{(1,1)}=\frac{13}{800}L\left(\frac{11}{288}\tau\right)+\frac{3}{32}L\left(\frac{3}{32}\tau\right)+\frac{3}{200}L\left(\frac{\tau}{8}\right),$$

$$M_{1\to1}^{(1,-1)}=M_{1\to1}^{(1,0)}=\frac{1}{8}L\left(\frac{35}{288}\tau\right),$$

$$M_{1\to1}^{(1,1)}=-\frac{5}{28}L\left(\frac{35}{288}\tau\right),\quad M_{1\to0}^{(1,-1)}=\frac{1}{8}L\left(\frac{\tau}{9}\right),$$

$$M_{1\to0}^{(1,0)}=M_{1\to0}^{(1,1)}=-\frac{1}{16}L\left(\frac{\tau}{9}\right). \tag{A1}$$

(ii) When $F_p=1$ and $F=2$,

$$M_{1\to2}^{(2,-2)}=0,\quad M_{1\to2}^{(2,-1)}=-\frac{3}{88}L\left(\frac{11}{288}\tau\right),$$

$$M_{1\to2}^{(2,0)}=-\frac{9}{352}L\left(\frac{11}{288}\tau\right)-\frac{1}{32}L\left(\frac{3}{32}\tau\right),$$

$$M_{1\to2}^{(2,1)}=-\frac{531}{8800}L\left(\frac{11}{288}\tau\right)-\frac{5}{96}L\left(\frac{3}{32}\tau\right)-\frac{1}{200}L\left(\frac{\tau}{8}\right),$$

$$M_{1\to2}^{(2,2)}=-\frac{21}{400}L\left(\frac{11}{288}\tau\right)-\frac{5}{48}L\left(\frac{3}{32}\tau\right)-\frac{1}{100}L\left(\frac{\tau}{8}\right),$$

$$M_{1\to1}^{(2,-2)}=0,\quad M_{1\to1}^{(2,-1)}=-\frac{3}{280}L\left(\frac{35}{288}\tau\right),$$

$$M_{1\to1}^{(2,0)}=-\frac{1}{56}L\left(\frac{35}{288}\tau\right),$$

$$M_{1\to1}^{(2,1)}=M_{1\to1}^{(2,2)}=-\frac{3}{140}L\left(\frac{35}{288}\tau\right),$$

$$M_{1\to0}^{(2,m)}=0\quad \text{for } m=-2,\ldots,2. \tag{A2}$$

(iii) When $F_p=2$ and $F=2$,

$$M_{2\to3}^{(2,-2)}=\frac{1}{8}L\left(\frac{7}{225}\tau\right),$$

$$M_{2\to3}^{(2,-1)}=\frac{1}{22}L\left(\frac{7}{225}\tau\right)+\frac{7}{88}L\left(\frac{2}{25}\tau\right),$$

$$M_{2\to3}^{(2,0)}=\frac{87}{1760}L\left(\frac{7}{225}\tau\right)+\frac{21}{176}L\left(\frac{2}{25}\tau\right)-\frac{7}{160}L\left(\frac{3}{25}\tau\right),$$

$$M_{2\to3}^{(2,1)}=\frac{17}{220}L\left(\frac{7}{225}\tau\right)+\frac{81}{176}L\left(\frac{2}{25}\tau\right)+\frac{21}{40}L\left(\frac{3}{25}\tau\right)-\frac{15}{16}L\left(\frac{\tau}{9}\right),$$

$$M_{2\to3}^{(2,2)}=\frac{5}{16}(1+K\delta_{1,q})L(s_0)-\frac{523}{1760}L\left(\frac{7}{225}\tau\right)-\frac{29}{44}L\left(\frac{2}{25}\tau\right)-\frac{77}{160}L\left(\frac{3}{25}\tau\right)+\frac{15}{16}L\left(\frac{\tau}{9}\right),$$

$$M_{2\to2}^{(2,-2)}=\frac{1}{8}L\left(\frac{5}{72}\tau\right),$$

$$M_{2\to2}^{(2,-1)}=\frac{1}{28}L\left(\frac{5}{72}\tau\right)+\frac{5}{56}L\left(\frac{3}{32}\tau\right),$$

$$M_{2\to2}^{(2,0)}=\frac{3}{28}L\left(\frac{5}{72}\tau\right)+\frac{1}{56}L\left(\frac{3}{32}\tau\right),$$

$$M_{2\to2}^{(2,1)}=\frac{211}{980}L\left(\frac{5}{72}\tau\right)-\frac{6}{49}L\left(\frac{3}{32}\tau\right),$$

$$M_{2\to2}^{(2,2)}=-\frac{257}{1960}L\left(\frac{5}{72}\tau\right)+\frac{19}{588}L\left(\frac{3}{32}\tau\right),$$

$$M_{2\to1}^{(2,-2)}=\frac{1}{8}L\left(\frac{9}{200}\tau\right),$$

$$M_{2\to1}^{(2,-1)}=-\frac{1}{68}L\left(\frac{9}{200}\tau\right)+\frac{19}{136}L\left(\frac{19}{800}\tau\right),$$

$$M_{2\to1}^{(2,0)}=-\frac{39}{18\,020}L\left(\frac{9}{200}\tau\right)-\frac{57}{3808}L\left(\frac{19}{800}\tau\right)+\frac{8437}{59\,360}L\left(\frac{59}{7200}\tau\right),$$

$$M_{2\to1}^{(2,1)}=\frac{139}{324\,360}L\left(\frac{9}{200}\tau\right)-\frac{27}{3808}L\left(\frac{19}{800}\tau\right)-\frac{429}{59\,360}L\left(\frac{59}{7200}\tau\right),$$

$$M_{2\to1}^{(2,2)} = \frac{13}{324\,360}L\left(\frac{9}{200}\tau\right) + \frac{1}{1904}L\left(\frac{19}{800}\tau\right) - \frac{429}{29\,680}L\left(\frac{59}{7200}\tau\right). \quad \text{(A3)}$$

(iv) When $F_p=2$ and $F=1$,

$$M_{2\to3}^{(1,m)} = 0 \quad \text{for } m=-1,0,1,$$

$$M_{2\to2}^{(1,-1)} = -\frac{3}{70}L\left(\frac{5}{72}\tau\right) - \frac{5}{504}L\left(\frac{3}{32}\tau\right),$$

$$M_{2\to2}^{(1,0)} = -\frac{3}{28}L\left(\frac{5}{72}\tau\right) - \frac{23}{504}L\left(\frac{3}{32}\tau\right),$$

$$M_{2\to2}^{(1,1)} = \frac{17}{441}L\left(\frac{3}{32}\tau\right) - \frac{99}{490}L\left(\frac{5}{72}\tau\right),$$

$$M_{2\to1}^{(1,-1)} = -\frac{25}{459}L\left(\frac{9}{200}\tau\right) - \frac{25}{408}L\left(\frac{19}{800}\tau\right),$$

$$M_{2\to1}^{(1,0)} = -\frac{5615}{97\,308}L\left(\frac{9}{200}\tau\right) + \frac{25}{11\,424}L\left(\frac{19}{800}\tau\right) - \frac{715}{11\,872}L\left(\frac{59}{7200}\tau\right),$$

$$M_{2\to1}^{(1,1)} = \frac{695}{194\,616}L\left(\frac{9}{200}\tau\right) - \frac{225}{3808}L\left(\frac{19}{800}\tau\right) - \frac{715}{11\,872}L\left(\frac{59}{7200}\tau\right). \quad \text{(A4)}$$

[1] W. Demtröder, *Laser Spectroscopy* (Springer, Berlin, 1998).
[2] O. Schmidt, K. M. Knaak, R. Wynands, and D. Meschede, Appl. Phys. B: Lasers Opt. **59**, 167 (1994).
[3] D. A. Smith and I. G. Hughes, Am. J. Phys. **72**, 631 (2004).
[4] C. Wieman and T. W. Hänsch, Phys. Rev. Lett. **36**, 1170 (1976).
[5] M. L. Harris, C. S. Adams, S. L. Cornish, I. C. McLeod, E. Tarleton, and I. G. Hughes, Phys. Rev. A **73**, 062509 (2006).
[6] H. J. Metcalf and P. van der Straten, *Laser Cooling and Trapping* (Springer, New York, 1999).
[7] K. B. MacAdam, A. Steinbach, and C. E. Wieman, Am. J. Phys. **60**, 1098 (1992).
[8] M. Pinard, C. G. Aminoff, and F. Laloë, Phys. Rev. A **19**, 2366 (1979).
[9] P. G. Pappas, M. M. Burns, D. D. Hinshelwood, M. S. Feld, and D. E. Murnick, Phys. Rev. A **21**, 1955 (1980).
[10] S. E. Harris, Phys. Today **50**, 36 (1997).
[11] M. Fleischhauer, A. Imamoglu, and J. P. Marangos, Rev. Mod. Phys. **77**, 633 (2005).
[12] E. Arimondo, Prog. Opt. **35**, 257 (1996).
[13] S. E. Harris, Phys. Rev. Lett. **62**, 1033 (1989).
[14] A. S. Zibrov, M. D. Lukin, L. Hollberg, D. E. Nikonov, M. O. Scully, H. G. Robinson, and V. L. Velichansky, Phys. Rev. Lett. **76**, 3935 (1996).
[15] D. F. Phillips, A. Fleischhauer, A. Mair, R. L. Walsworth, and M. D. Lukin, Phys. Rev. Lett. **86**, 783 (2001).
[16] M. Fleischhauer and M. D. Lukin, Phys. Rev. A **65**, 022314 (2002).
[17] S. Banerjee and V. Natarajan, Opt. Lett. **28**, 1912 (2003).
[18] D. J. Fulton, S. Shepherd, R. R. Moseley, B. D. Sinclair, and M. H. Dunn, Phys. Rev. A **52**, 2302 (1995).
[19] S. J. Park, H. S. Lee, H. Cho, and J. D. Park, J. Korean Phys. Soc. **33**, 281 (1998).
[20] V. Wong, R. W. Boyd, C. R. Stroud, Jr., R. S. Bennink, and A. M. Marino, Phys. Rev. A **68**, 012502 (2003).
[21] S. Chakrabarti, A. Pradhan, A. Bandyopadhyay, A. Ray, B. Ray, N. Kar, and P. N. Ghosh, Chem. Phys. Lett. **399**, 120 (2004).
[22] S. Chakrabarti, A. Pradhan, B. Ray, and P. N. Ghosh, J. Phys. B **38**, 4321 (2005).
[23] F. Magnus, A. L. Boatwright, A. Flodin, and R. C. Shiell, J. Opt. B: Quantum Semiclassical Opt. **7**, 109 (2005).
[24] A. Narayanan, Eur. Phys. J. D **39**, 13 (2006).
[25] D. Bhattacharyya, B. Ray, and P. N. Ghosh, J. Phys. B **40**, 4061 (2007).
[26] D. Bhattacharyya, A. Bandyopadhyay, S. Chakrabarti, B. Ray, and P. N. Ghosh, Chem. Phys. Lett. **440**, 24 (2007).
[27] S. Chakrabarti, B. Ray, and P. N. Ghosh, Eur. Phys. J. D **42**, 359 (2007).
[28] G. Moon and H. R. Noh, J. Opt. Soc. Am. B **25**, 701 (2008).
[29] H. D. Do, M. S. Heo, G. Moon, H. R. Noh, and W. Jhe, Opt. Commun. **281**, 4042 (2008).
[30] D. Meschede, *Optics, Light and Lasers* (Wiley-VCH, Weinheim, 2007).
[31] A. R. Edmonds, *Angular Momentum in Quantum Mechanics* (Princeton University Press, Princeton, N. J., 1960).
[32] J. Sagle, R. K. Namiotka, and J. Huennekens, J. Phys. B **29**, 2629 (1996).
[33] R. Grimm and J. Mlynek, J. Opt. Soc. Am. B **5**, 1655 (1988).
[34] R. Grimm and J. Mlynek, Phys. Rev. Lett. **63**, 232 (1989).